Developmental and Comparative Immunology 52 (2015) 123–131

Contents lists available at ScienceDirect

Developmental and Comparative Immunology

journal homepage: www.elsevier.com/locate/dci

LFP-20, a porcine lactoferrin peptide, ameliorates LPS-induced inflammation via the MyD88/NF-κB and MyD88/MAPK signaling pathways

Xin Zong, Deguang Song, Tenghao Wang, Xi Xia, Wangyang Hu, Feifei Han, Yizhen Wang *

Key Laboratory of Animal Nutrition and Feed Science in Eastern China, Ministry of Agriculture, College of Animal Sciences, Zhejiang University, Hangzhou 310058, China

ARTICLE INFO

Article history:
Received 7 April 2015
Revised 17 May 2015
Accepted 18 May 2015
Available online 21 May 2015

Keywords:
LFP-20
Lipopolysaccharide
Inflammation
MyD88
NF-κB
MAPK

ABSTRACT

LFP-20 is one of the 20 amino acid anti-microbial peptides identified in the N terminus of porcine lactoferrin. Apart from its extensively studied direct anti-bacterial activity, its potential as an activator of immune-related cellular functions is unknown. Therefore, this study investigated its anti-inflammatory effects in lipopolysaccharide (LPS)-stimulated pig alveolar macrophages *in vitro* and systemic inflammation in an *in vivo* mouse model. We found that the inhibitory effects of LFP-20 on production of pro-inflammatory cytokines were independent of its LPS-binding activity. However, they were associated with NF-κB and MAPK-dependent signaling. Furthermore, LFP-20 might directly influence MyD88 levels to block its interaction with NF-κB and MAPK-dependent signaling molecules that might alter LPS-mediated inflammatory responses in activated macrophages. Taken together, our data indicated that LFP-20 prevents the LPS-induced inflammatory response by inhibiting MyD88/NF-κB and MyD88/MAPK signaling pathways, and sheds light on the potential use of LFP-20 in the therapy of LPS-mediated sepsis.

1. Introduction

Inflammation is a defensive response of living tissues against harmful stimuli, such as pathogens, damaged cells, or irritants (Diao et al., 2014). The mechanism that underlies such phenomenon may be reflected in the context of the activation of monocytes and macrophages, which secrete an array of pro-inflammatory mediators such as cytokines, chemokines and cytoplasmic or nuclear signaling proteins. Increasing evidence has indicated that dysregulated activation of inflammation is one of the principal causes of non-communicable chronic diseases like cardiovascular disease, atherosclerosis, cancer, obesity and insulin resistance (Balkwill and Mantovani, 2001; Libby, 2006).

The classic model used to induce inflammation is the macrophage stimulated by lipopolysaccharide (LPS), a key component of Gram-negative bacterial cell walls. LPS activates several signaling cascades driving the expression of pro-inflammatory cytokines, such as tumor necrosis factor-alpha (TNF-α), interleukin-1 (IL-1), and interleukin-6 (IL-6) (Lee et al., 2013), through binding to its cognate receptors CD14 and Toll-like receptors that are expressed at the cell surface (Medzhitov, 2001). These cytokines activate innate immunity, but their over-expression causes acute phase endotoxemia, which might lead to septic shock, tissue injury and even death. Therefore, regulation of inflammatory cytokine release is potentially beneficial to prevent chronic disease-associated inflammation (O'Keefe et al., 2008).

Toll-like receptor 4 (TLR4) is a pattern recognition and "immunological danger" sensing receptor that connects innate and adaptive immune responses, and is an essential co-receptor for LPS with CD14 (Du et al., 1999). There are two different signaling pathways that are involved in cell-mediated responses to LPS. The first is the myeloid differentiation factor-88 (MyD88)-dependent pathway, and the second is the TIR domain-containing adaptor inducing interferon-β (TRIF)-dependent pathway; both of which are triggered by the association of LPS and TLR4. Activation of the MyD88-dependent pathway leads to phosphorylation of mitogen-activated protein (MAP) kinase, IκB kinase (IKK) and nuclear factor κB (NF-κB), eventually contributing to the expression of pro-inflammatory cytokines (Kawai et al., 1999). The TRIF-dependent pathway activates the interferon-regulatory factor-1 (IRF-3) transcription factor that leads to induction of IFN-β and IFN-inducible genes (Hoebe et al., 2003; Yamamoto et al., 2003). NF-κB is a transcription factor that plays a critical role in the regulation of gene expression associated with many cellular processes.

When stimulated with LPS, IκBs, and inhibitory proteins of NF-κB, are phosphorylated by IKK, thereby allowing activated NF-κB

* Corresponding author. Institute of Feed Science, Zhejiang University, 866 Yuhangtang Road, Hangzhou 310058, China. Tel.: +86 571 88982815; fax: +86 57188982650.
E-mail address: yzwang321@zju.edu.cn (Y. Wang).

http://dx.doi.org/10.1016/j.dci.2015.05.006
0145-305X/

to translocate to the nucleus (Chen and Lin, 2001). MAPK-dependent signal transduction pathways are among the most widespread mechanisms of eukaryotic cell regulation. MAPK cascades that converge on c-Jun N-terminal kinases (JNK) and p38 MAPKs are recognized as regulators of inflammation that could be up-regulated in fibroblastic and macrophage-like cell-lines (Kyriakis and Avruch, 2001; Scherle et al., 1998).

LFP-20 is one of the 20 amino acid anti-microbial peptides that were identified in the N-terminus of lactoferrin (LF), which is a member of the porcine LF family. Its three-dimensional structure is shown in Fig. 1A. Previous studies reported that cationic peptides that were isolated after degradation of bovine and human lactoferrin by gastric pepsin displayed higher anti-microbial activity than their native protein counterparts. These peptide fragments were named bovine LF (LFB) and human LF (LFH) and they exerted anti-microbial activities against a broad spectrum of microorganisms, including gram-positve and gram-negative bacteria, and fungi (Bellamy et al., 1992, 1993; Tomita et al., 1991). In contrast to the bovine and human lactoferrin peptide, which have been studied for at least twenty years, porcine lactoferrin peptide was less well-studied. Chen et al. identified anti-microbial effects of LFP-20 on *Escherichia coli*, *Staphylococcus aureus*, and *Candida albicans* (Chen et al., 2006). Our previous study identified key amino acids in the LFP-20 sequence using amino acid substitutions and activity assays (Han et al., 2013). Much research has focused on the anti-microbial functions of LFP-20. By contrast, their potential to activate immune-related cellular functions and modulators of the host immune response to endogenous or exogenous mediators has not been well studied.

In this study, we attempted to clarify the anti-inflammatory mechanisms of LFP-20 by thoroughly exploring the molecular basis of its anti-inflammatory effects, using LPS-induced pig alveolar macrophages and a murine model of systemic LPS-induced inflammation.

2. Materials and methods

2.1. Peptide synthesis

LFP-20 (KCRQWQSKIRRTNPIFCIRR) was chemically synthesized by standard solid-phase procedures with 9-fluorenylmethoxycarbonyl (Fmoc) using an Apex 396 peptide synthesizer (Aapptec, Louisville, KY, USA). Ninety-five percent purity of synthetic peptides was achieved and verified using Agilent 1200 Series high-performance liquid chromatography (Agilent Technologies, Santa Clara, CA, USA) and a Thermo Finnigan LCQ ion trap mass spectrometer (Thermo Finnigan, San Jose, CA, USA). The synthetic peptide was dissolved in endotoxin-free water and stored at –80 °C.

2.2. Regents

Ultrapure LPS from *Escherichia coli* strain O111:B4 and polymyxin B were purchased from Sigma-Aldrich (St. Louis. MO, USA). TLR4 (ab8376) was purchased from Abcam (Abcam, Cambridge, MA, USA); IKK-β (2678) and p-IKK-β (2697) were purchased from Cell Signaling Technology (Cell Signaling Technology, Danvers, MA, USA); MyD88 (sc11356), IκB-α (sc371), p-IκB-α (sc8404), NF-κB (p65) (sc7151), NF-κB (p-p65) (sc33020), p38 (sc728), c-Jun (sc1694), p-c-Jun (sc822), GAPDH (sc48166) or β-actin (sc47778) antibody were purchased from Santa Cruz Biotechnology, Inc. (Santa Cruz, CA, USA). Secondary antibodies were purchased from HuaAn (HuaAn, Hangzhou China).

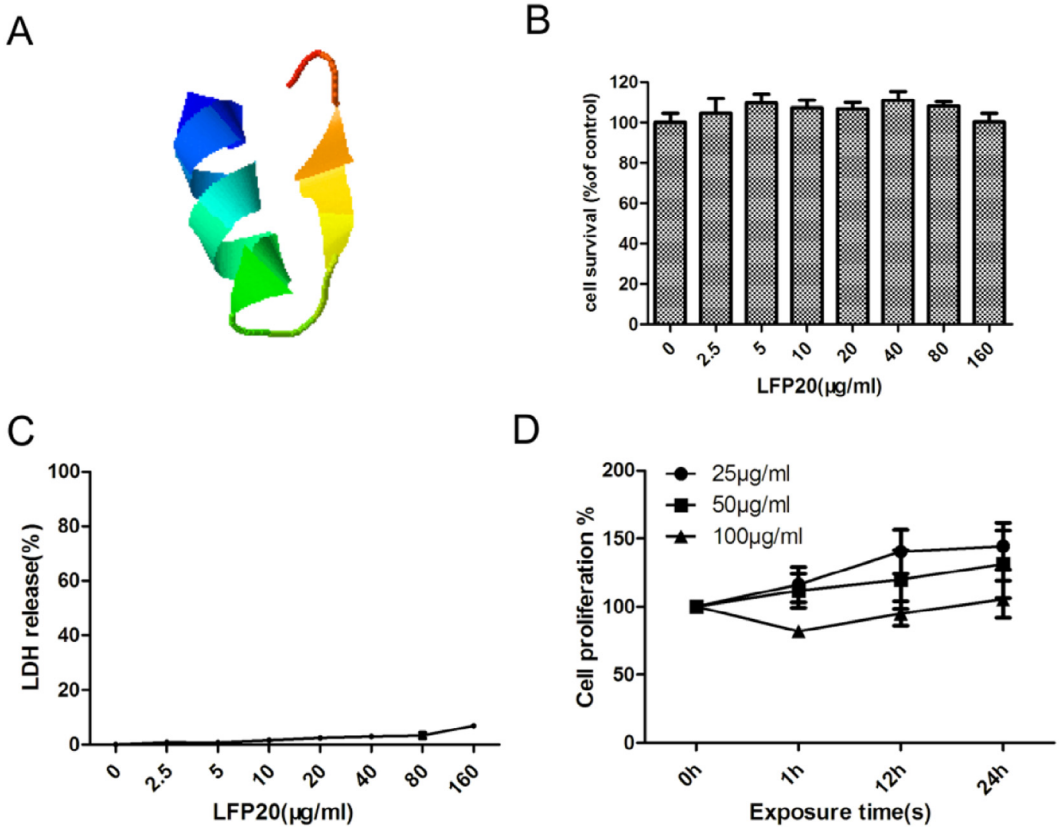

Fig. 1. The structure of LFP-20 and incidence of LFP-20 exposure on pig alveolar macrophage cell viability and cytotoxicity. (A) Three-dimensional structure of LFP-20; (B) activity of LFP-20 toward pig alveolar macrophages cell viability as determined by MTT assay; (C) activity of LFP-20 toward pig alveolar macrophage extracellar LDH release; (D) activity of LFP-20 toward pig alveolar macrophage cell viability assay by WST-1 assay. Results are given as mean ± SEM. Differences between groups were determined by one-way ANOVA followed by Duncan's post-hoc analysis (n = 6).

2.3. Cell culture and stimulation

The pig alveolar macrophage cell-line 3D4/2 (Weingartl et al., 2002) was purchased from the CBCAS (Cell Bank of the Chinese Academy of Sciences, Shanghai, PR China), and were cultured in RPMI-1640 medium (Invitrogen) that was supplemented with 10% (v/v) fetal bovine serum (Hyclone) and antibiotics (100 U/mL penicillin and 100 μg/mL streptomycin sulfate) (Hyclone) at 37 °C in a fully-humidified 5% CO_2 in air incubator.

Cells analyzed for cytokine gene expression and quantification in cell culture supernatants were seeded in 6-well plates at a density of 1.8×10^6 cells per well and cultured overnight before being stimulated with LPS (1 μg/mL) in the absence or presence of LFP-20 at the indicated concentrations. In some experiments, cells were pretreated with LFP-20 or polymyxin B and then rinsed (or not) extensively with complete medium before addition of LPS, or prestimulated for 3 h with LPS and rinsed as described earlier before addition of LFP-20 at the indicated concentrations.

2.4. Animal model

Male 6- to 8-wk-old C57BL/6 mice were obtained from the Laboratory Animal Center of Zhejiang University (Hangzhou, PR China) and maintained in plastic cages under standard conditions. Diet and drinking water were provided *ad libitum*. Animal studies were approved by the Institutional Animal Care and Use Committee of Zhejiang University and performed in accordance with institutional guidelines.

All the mice had free access to water and food throughout the experiment. The mice were randomly divided into 6 groups of 12 mice per group (Table 1): control, LFP-20-treated, LPS-treated, 2.5 mg/kg LFP-20 pretreated followed by LPS treated (LFPL + LPS), 5 mg/kg LFP-20 pretreated followed by LPS treated (LFPM + LPS), 10 mg/kg LFP-20 pretreated followed by LPS treated (LFPH + LPS).

Different concentrations of LFP-20 were injected intraperitoneally (i.p.) into C57BL/6 male mice once per day for 6 days, whereas the control and LPS-treated groups were i.p. injected with an equal volume of sterile saline. On day 6, mice in the LPS and LFP-20 (12.5, 25, and 50 μg/mL) plus LPS groups were i.p. injected with LPS (10 mg/kg mouse weight) 1 h after LFP-20 or saline treatment; the other groups were injected with an equal volume of saline. All mice were sacrificed 6 h after i.p. injection of LPS or saline. Blood was centrifuged at 3000 rpm for 10 mins, and then the serum was collected and assayed as will be described later.

2.5. Prediction of three-dimensional structure

Three-dimensional structures of LFP-20 were predicted by I-TAEER (http://zhanglab.ccmb.med.umich.edu/I-TASSER/).

Table 1
Experimental design with different treatment groups.

Groups[a]	control	LFP-20	LPS	LFPL+LPS	LFPM+LPS	LFPH+LPS
Treatment 1[b]	PBS	LFP-20	PBS	LFP-20	LFP-20	LFP-20
Treatment 2[c]	PBS	LFP-20	LPS	LPS	LPS	LPS

Abbreviations: LPS, lipopolysaccharide; PBS, phosphate buffer saline.

[a] Seventy-two C57/BL6 male mice weighing 18–21 g (6–8 weeks old) were randomly distributed to six groups: control, LFP-20-treated, LPS-treated, 2.5 mg/kg LFP-20 pretreated followed by LPS treated (LFPL + LPS), 5 mg/kg LFP-20 pretreated followed by LPS treated (LFPM + LPS), 10 mg/kg LFP-20 pretreated followed by LPS treated (LFPH + LPS). The dosage of LPS was 10 mg/kg mouse weight.

[b] Treatment 1: mice were supplied with PBS or LFP-20 solution for 6 days.

[c] Treatment 2: mice got intraperitoneally injection of PBS, LFP-20 solution or LPS solution for 6 hours, then all mice were sacrificed.

2.6. Determination of cytokine secretion

The levels of cytokines (*e.g.*, TNF-α, IL-6 and IL-1β) in the supernatants were quantified using a commercially available enzyme-linked immunosorbent assay (ELISA) kits (Raybiotech, USA), which was porcine specific according to the manufacturer's instructions. The levels of cytokines (*e.g.*, TNF-α, IL-6 and IL-1β) in the serum were quantified by commercial ELISA kits (Raybiotech, USA), which were specific for murine specimens according to the manufacturer's instructions.

2.7. Cell viability assay

The inhibitory effects of LFP-20 on porcine alveolar macrophages were evaluated using the cell proliferation reagent WST-1 (Roche Applied Science, Mannheim, Germany). In 96-well plates, pig alveolar macrophages (at a density of 2×10^4 cells/well) were resuspended in RPMI 1640 medium supplemented with 10% heat inactivated fetal bovine serum and incubated at 37 °C in 5% CO2 in air for 2 h. Next, various concentrations of peptides were added to a final volume of 100 μL. After 18 h incubation at 37 °C under 5% CO2 in air, 10 μL of WST-1 reagent was added to each well and samples were further incubated for 60 min. Absorbance of the colored formazan product was measured using an automated microplate reader (Lambda E, MWG Biotech, Ebersberg, Germany) at a wavelength of 450 nm, using 900 nm as a reference wavelength. The mean absorbance of control wells (*i.e.*, cells without peptides) represented 100% cell viability.

Cell viability was also determined in an MTT assay, which is based on 3-(4, 5-dimethylthiazol-2-yl)-2, 5-diphenyltetrazolium bromide uptake into cells and mitochondrial enzyme activity. Briefly, pig alveolar macrophages were seeded into 96-well plates at a density of 2×10^4 cells per well 24 h before treatment. Cells were treated with various concentrations of LFP-20 for 24 h followed by incubation with 5 mg/mL of MTT working solution for 4 h at 37 °C. After adding 100 μL of DMSO to dissolve the crystals, the absorbance value of each well was measured at 570 nm using an automated microplate reader (Lambda E, MWG Biotech, Ebersberg, Germany). Three replicates were carried out for each of the different treatments.

2.8. Lactate dehydrogenase release assay for cytotoxicity (LDH)

To detect direct peptide-induced cell lysis, we performed lactate dehydrogenase (LDH) release (Roche Applied Science) according to the manufacturer's instructions. The pig alveolar macrophages were seeded in 96-well plates for 2 h and incubated with various concentrations of peptides for another 1, 12, 24 h at 37 °C under a 5% CO_2 in air atmosphere. Cells were treated with 2% (vol/vol) Triton X-100 for 10 min before running the assay as a positive control for maximal LDH release. Untreated cells served as controls for spontaneous LDH release. Supernatants were removed and centrifuged at $800 \times g$ for 10 min to remove contaminating cells. Aliquots of assay culture supernatants were treated with enzymatic assay reagent for 30 min. Absorbance values were subsequently measured in a microplate reader at 490 nm, using 900 nm as a reference wavelength. Specific LDH release was calculated using the following formula: %LDH release = $100 \times$ (Exp-Spo)/(Max-Spo), with Exp representing experimental release, Spo representing baseline release, and Max representing maximum LDH release.

2.9. In vitro *LPS-binding*

A quantitative chromogenic end-point amebocyte lysate (CE LAL) assay was performed using the QCL-1000 kit (Xiamen, China). Incubations were performed using flat-bottom, non-pyrogenic 96-well

tissue culture plates. LFP-20 and polymyxin B dilutions were prepared in pyrogen-free water. Each peptide dilution was incubated in the presence/absence of LPS derived from *Escherichia coli strain O111:B4* (1.0 U/mL final concentration). Plates were maintained at 37 °C for 15 min to allow LPS binding and were then incubated at 37 °C for 6 min in the presence of LAL assay reagent. The release of *p*-nitroaniline was detected spectrophotometrically at 405 nm between 0 and 6 min. Standard curves that were generated with increasing amounts of LPS were linear between 0.1 and 1.0 endotoxin units/assay.

2.10. Transient transfection of small RNA interference (siRNA)

Small-interfering RNA that specifically targeted pig MyD88 were designed and synthesized by Changsha Yingrun Biotechnology Co., Ltd. The pig alveolar macrophage cell-line 3D4/2 was cultured in 6-well plates at a density of 1.8×10^6 cells per well, and were then transfected with 1 μg/mL siRNA using Lipofectamine-2000 reagent (Invitrogen) according to the manufacturer's instructions. At 6 h post-transfection, the cells were treated with/without LFP-20, and /or LPS at indicated concentrations.

2.11. Reverse transcription-quantitative real-time PCR (RT-PCR) analysis

Total RNA was isolated from pig alveolar macrophage cells using TRIzol (Invitrogen) according to the manufacturer's instructions. One microgram of total RNA was reverse transcribed using the MMLV Reverse Transcriptase (Thermo scientific, USA) following the supplier's protocol. The reactions were incubated at 25 °C for 20 min, then at 42 °C for 60 min, and finally terminated at 70 °C for 10 min. Real-time PCR reactions were conducted in triplicate on a Step one Real-Time PCR System (ABI Step one Plus, Applied Biosystems, Foster City, CA, USA) using FastStrat Universal SYBR Green Master (ROX) (Roche, USA). The PCR primer sequences were designed from

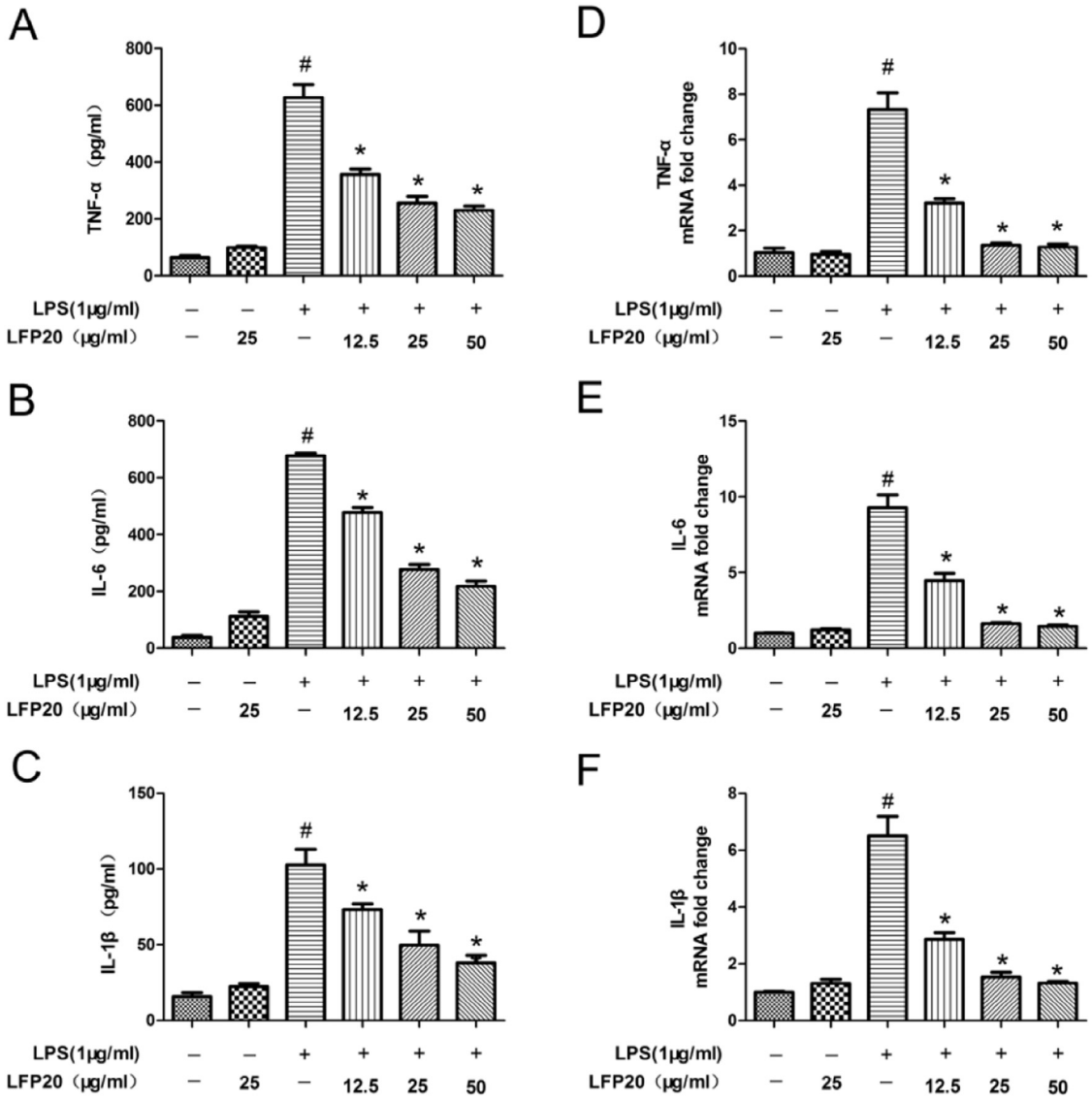

Fig. 2. LFP-20 inhibited LPS-induced gene and protein expression of pro-inflammatory cytokines in pig alveolar macrophages. The effect on protein expression (A–C) and gene expression (D–F) of TNF-α, IL-6, and IL-1β in LPS-stimulated pig alveolar macrophages. The pig alveolar macrophage cell-line 3D4/2 was incubated for 3 h with medium only or 1 μg/mL LPS in the absence/presence of LFP-20 (at concentrations of 12.5, 25, or 50 μg/mL). TNF-α, IL-6 and IL-1β in culture supernatants were measured by ELISA, and transcript levels were determined by RT-PCR. Results are given as mean ± SEM. Differences between groups were determined by one-way ANOVA followed by Duncan's post-hoc analysis (n = 3). $^{\#}p < 0.05$ as compared to the control group, and $^{*}p < 0.05$ as compared to the LPS-treated group.

Table 2
Primers for real-time PCR.

Primer name	Primer sequence (5′→3′)	Tm (°C)	Accession number
TNF-α	F: 5′-CGA CTCAGTGCCGAGATCAA-3′ R: 5′-CCTGCCCAGATTCAGCAAAG-3′	60	X57321
IL-6	F: 5′-TGGATAAGCTGCAGTCACAG-3′ R: 5′-ATTATCCGAATGGCCCTCAG-3′	60	M86722
IL-1β	F: 5′-GCCCTGTACCCCAACTGGTA-3′ R: 5′-CCAGGAAGACGGGCTTTTG-3′	60	M86725
18s	F: 5′-CCCACGGAATCGAGAAAGAG-3′ R: 5′-TTGACGGAAGGGCACCA-3′	60	AY265350

The sequences in Table 2 are available through GenBank (http://www.ncbi.nlm.nih.gov/nuccore/) under the accession numbers listed above.
F, forward; R, reverse.

reported sequences (Moue et al., 2008) and are listed in Table 2. Real-time PCR reactions were performed as follows: a precycling stage at 95 °C for 30 s, then 40 cycles of denaturation at 95 °C for 10 s and an annealing step at 60 °C for 34 s. Fluorescence was measured at the end of each annealing step, and the melting curves were monitored to confirm the specificity of the PCR amplicon. The $2^{-\Delta\Delta CT}$ method was used to determine mRNA expression levels (Livak and Schmittgen, 2001).

2.12. Western blot analysis

The porcine alveolar macrophage 3D4/2 cell-line was cultured in 6-well plates at a density of 1.8×10^6 cells per well, and were then stimulated with LPS (1 μg/mL) in the presence/absence of LFP-20, following which they were lysed. The whole protein was obtained using the Whole Protein Extraction Kit (KeyGEN Biotech, Nanjing, China) according to the manufacturer's instructions. Protein concentrations were determined with the BCA Assay Kit (KeyGEN Biotech. Nanjing, China). Next, 40 μg of total protein of each specimen was separated by 10% SDS–PAGE, which were then transferred onto polyvinylidene difluoride membranes (PVDF). The membranes were then blocked with 5% non-fat dried-milk proteins in 0.05% TBST, then probed with TLR4, MyD88, IKK-β, p-IKK-β, IκB-α, p-IκB-α, p65, p-p65, p38, c-Jun, p-c-Jun, GAPDH or β-actin specific monoclonal antibodies. After washing with TBST, proteins were detected with HRP-conjugated secondary antibodies (Hua An, Hangzhou China) for 1 h. Specific bands were visualized with an ECL detection kit (Santa Cruz Biotechnology, Inc., CA, USA). Image J software was used to quantify the density of each of the specific protein bands.

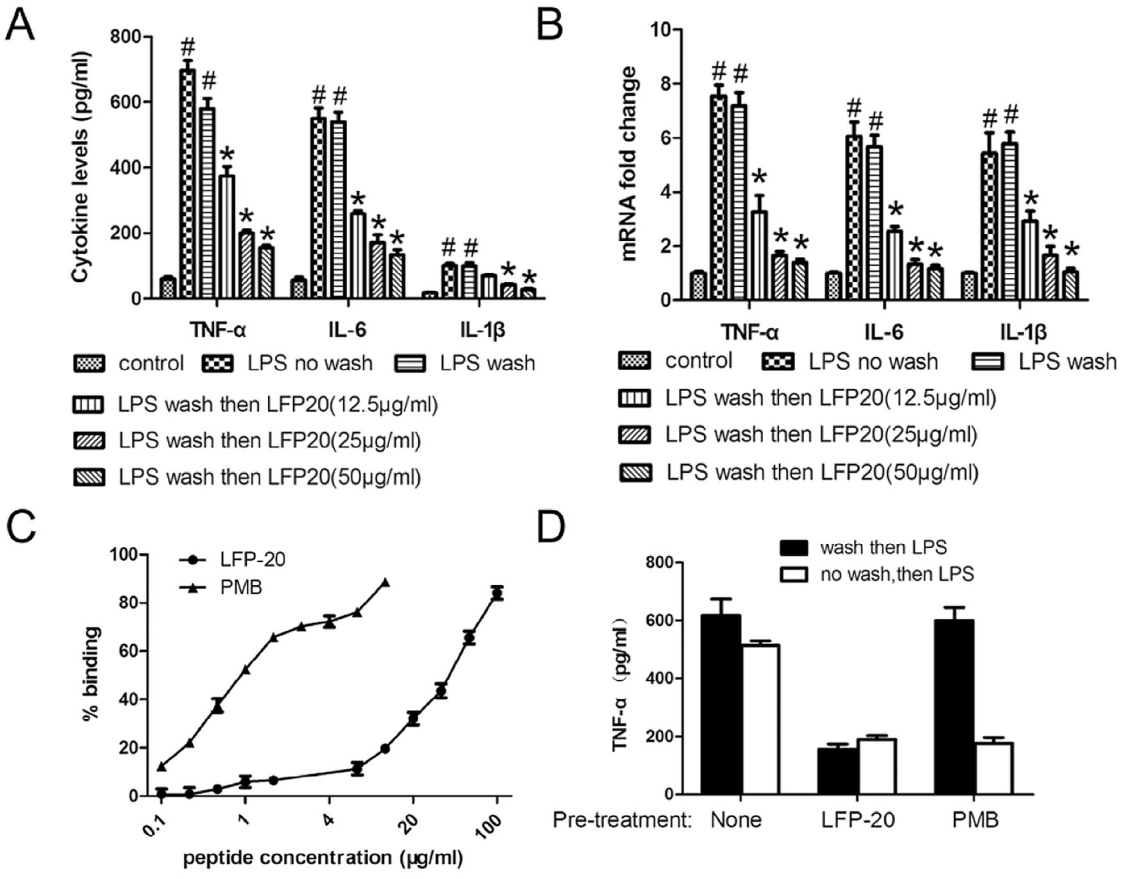

Fig. 3. LFP-20 affects LPS-induced cytokine gene and protein expression independently of its LPS-binding activity. Effect on protein (A) and gene expression (B) of TNF-α, IL-6, and IL-1β in pig alveolar macrophages. The pig alveolar macrophage cell-line 3D4/2 was incubated for 3 h with medium only or 1 μg/mL LPS, and then washed extensively and further incubated with LFP-20 (at concentrations of 12.5, 25, or 50 μg/mL) for another 3 h. (C) Binding of LFP-20 (closed circle) or polymyxin B (PMB, shown as triangles) binding to LPS was determined using the chromogenic *in vitro* LAL assay as described in Section 2. (D) The pig alveolar macrophage cell-line 3D4/2 was treated in serum-free medium only or 25 μg/mL LFP-20 or 10 μg/mL polymyxin B for 3 h, washed twice in PBS, then incubated with 1 μg/mL LPS for another 3 h. TNF-α, IL-6 and IL-1β in the culture supernatants were measured by ELISA, and transcript levels were determined by RT-PCR. Results are given as mean ± SEM. Differences between groups were determined by one-way ANOVA followed by Duncan's post-hoc analysis (n = 3). $^{\#}p < 0.05$ as compared to the control group, and $^{*}p < 0.05$ as compared to the LPS-treated group.

2.13. Statistical analysis

Data are presented as the mean ± SEM. Statistical evaluations were determined by using the GraphPad Prism version 5.01 software program (GraphPad Software, Inc., San Diego, CA, USA) by one-way analysis of variance (ANOVA), and post-hoc analysis by Duncan's test. An alpha value of $P < 0.05$ was considered statistically significant.

3. Results

3.1. LFP-20 inhibited LPS-induced expression of pro-inflammatory cytokines in pig alveolar macrophages

To determine the inhibitory effect of LFP-20 on the LPS-induced inflammatory response, protein and gene expression of pro-inflammatory cytokines (*e.g.*, TNF-α, IL-6, and IL-1β) were measured. The pig alveolar macrophage 3D4/2 cell-line was stimulated with LPS in the absence or presence of dose-dependent concentrations of LFP-20. Stimulation of pig alveolar macrophages with LPS led to a robust increase in the protein and gene expression of TNF-α, IL-6, and IL-1β. By contrast, cells that were treated with LPS in the presence of LFP-20 markedly decreased the expression of TNF-α, IL-6, and IL-1β in a dose-dependent manner (Fig. 2A–F).

Next, to determine the possibility that the cytotoxic susceptibility of LFP-20 cells resulted in the inhibitory effects against LPS-induced production of these cytokines, we assayed the cytotoxicity of LFP-20 independently with both MTT and WST-1 assay(s). The treatment of 3D4/2 cells with LFP-20 had no cytotoxic effect on cell viability under the concentrations used in these experiments, even under conditions where there was a tendency of increased cell proliferation at 25 μg/mL of LFB-20 according to the WST-1 assays (Fig. 1B, D). The release of the cytoplasmic enzyme LDH into the culture supernatants was also measured. LDH release was enhanced in a dose-dependent manner with increasing doses of LFP-20, but it had few effects on LDH release as compared with controls (Fig. 1C). This observation indicated that LFP-20 had no cytotoxic effects when LPS-induced inflammatory responses were suppressed in alveolar macrophages.

3.2. LFP-20 affects LPS-induced cytokine expression independently of its LPS-binding activity

To evaluate the contribution of direct LFP-20-LPS binding to the inhibition of LPS-induced inflammatory cytokines protein and gene

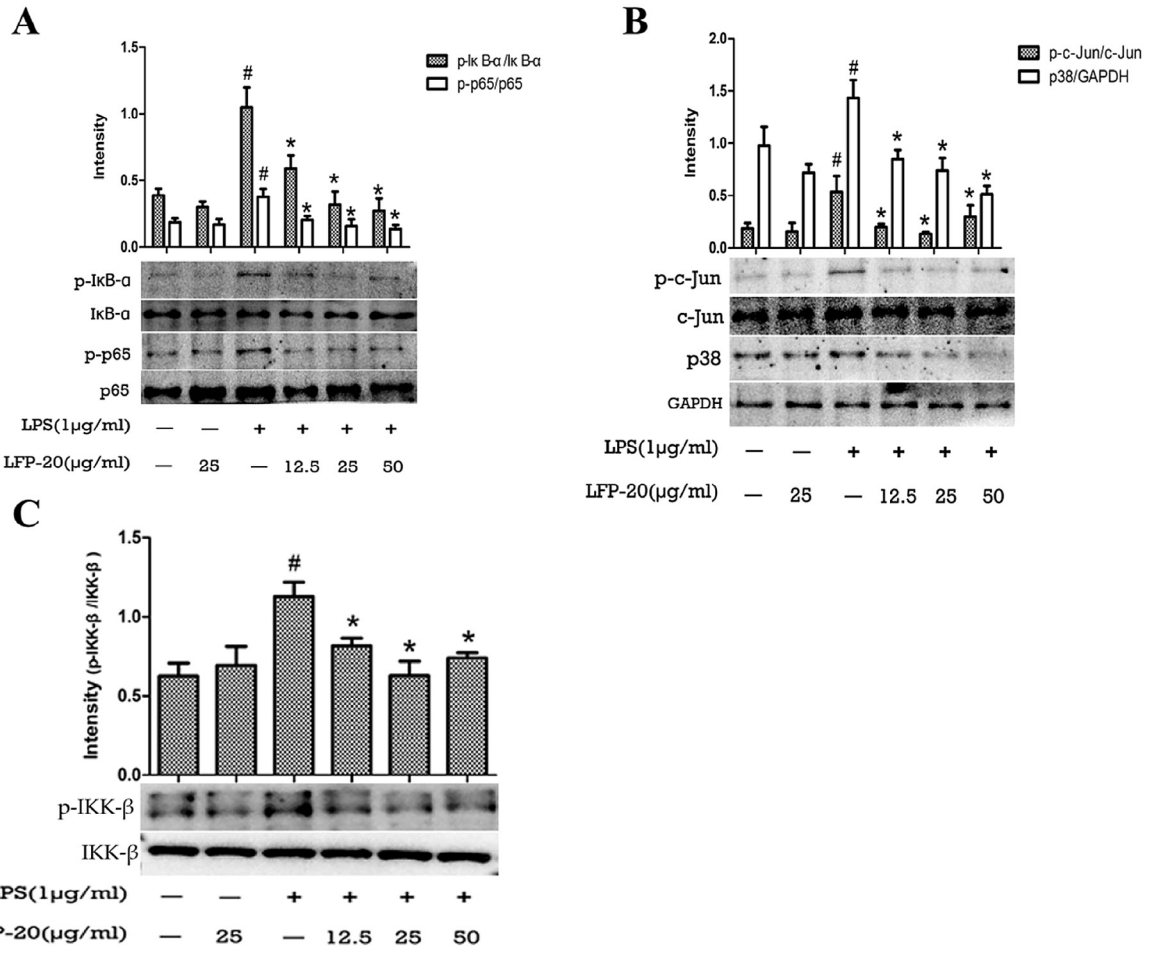

Fig. 4. LFP-20 inhibited LPS-induced NF-κB (p65) and MAPK (p38) signaling. (A) Effect of LFP-20 on LPS-activated NF-κB (p65) signaling. (B) Effect of LFP-20 on LPS-activated MAPK (p38) signaling. (C) Effect of LFP-20 on LPS-activated IKK-β phosphorylation. The pig alveolar macrophage cell-line 3D4/2 was incubated for 3 h with medium only or 1 μg/mL LPS in the absence or presence of LFP-20 (at concentrations of 12.5, 25, or 50 μg/mL). Protein expression was determined by Western blot assay. GAPDH was used as an internal house-keeping protein control. Image J software was used to quantify the density of the protein bands. Results are given as mean ± SEM. Differences between groups were determined by one-way ANOVA followed by Duncan's post-hoc analysis ($n = 3$). $^{\#}p < 0.05$ as compared to the control group, and $^{*}p < 0.05$ as compared to the LPS-treated group.

expression, we treated pig alveolar macrophages with LFP-20 prior to, or following LPS-mediated stimulation to minimize the possibility of direct binding between LFP-20 and LPS. The pattern of cytokine protein and gene expression in macrophages that were pretreated with LPS was detected in parallel and was similar to that determined in macrophages that were stimulated for 3 h with LPS in the presence of 25 μg/mL LFP-20 (Figs. 3A–B and 2A–F).

The ability of LFP-20 to neutralize LPS was evaluated by inhibiting the dose-dependent LPS-induced LAL clotting cascade. LFP-20 was 50-fold less potent than polymyxin B, a cyclic hydrophobic peptide known to bind LPS (Semple et al., 2011), and with 50% binding rate values of 50 μg/mL (LFP-20) and 1 μg/mL (polymyxin B) respectively (Fig. 3C). Next, we pig treated alveolar macrophages with LFP-20 or polymyxin B for 3 h and washed the cells thoroughly before stimulating with LPS (Fig. 3D). Removal of LFP-20 from the extracellular environment failed to alter the ability of LFP-20 to inhibit the production of pro-inflammatory cytokines that were induced by LPS. By contrast, the anti-inflammatory effect of polymyxin B was significantly decreased by washing. These results in combination with our previous finding that LFP-20 inhibited gene and protein expression profiles of pro-inflammatory cytokines, suggesting that other than neutralizing LPS through LFP-20-binding directly, most of the LFP-20 inhibitory effect occurs downstream of LPS-mediated TLR4 activation.

3.3. LFP-20 inhibited the activation of NF-κB and MAPK signaling in LPS-stimulated pig alveolar macrophages

NF-κB plays a critical role in inflammation by regulating the expression of many cytokines that primarily involve IL-6 and TNF-α (Korhonen et al., 2005). NF-κB is a complex of NF-κB–IκB-α in the cytoplasm, and its translocation is regulated by the phosphorylation of IKK-β (Wang et al., 2001). To study the possibility that the inhibitory effects of LFP-20 on pro-inflammatory cytokine production act through NF-κB signaling in LPS-induced alveolar macrophages, we determined the effect of LFP-20 on the translocation of NF-κB (p65). Cells that were treated with LPS in the presence of LFP-20 for 3 h stimulated significantly increased levels of NF-κB (p65) and Iκ-B-α phosphorylation, while cells that were incubated with LFP-20 provoked dampened levels of NF-κB (p65) and Iκ-B-α phosphorylation (Fig. 4A). To futher validate the effect of LFP-20 inhibiting NF-κB (p65) activation, we detected the levels of phospho-IKK-β. In agreement with the supressive effect of LFP-20 on the translocation of NF-κB (p65), the LPS-induced phosphorylation of IKK-β was attenuated by LFP-20 in a dose-dependent manner (Fig. 4C).

We also investigated the effect of LFP-20 on LPS-induced activation of MAPKs (*i.e.*, p38-MAP kinases and c-Jun). The level of phospho-c-Jun and p38 MAP kinases in cells treated with LPS in the

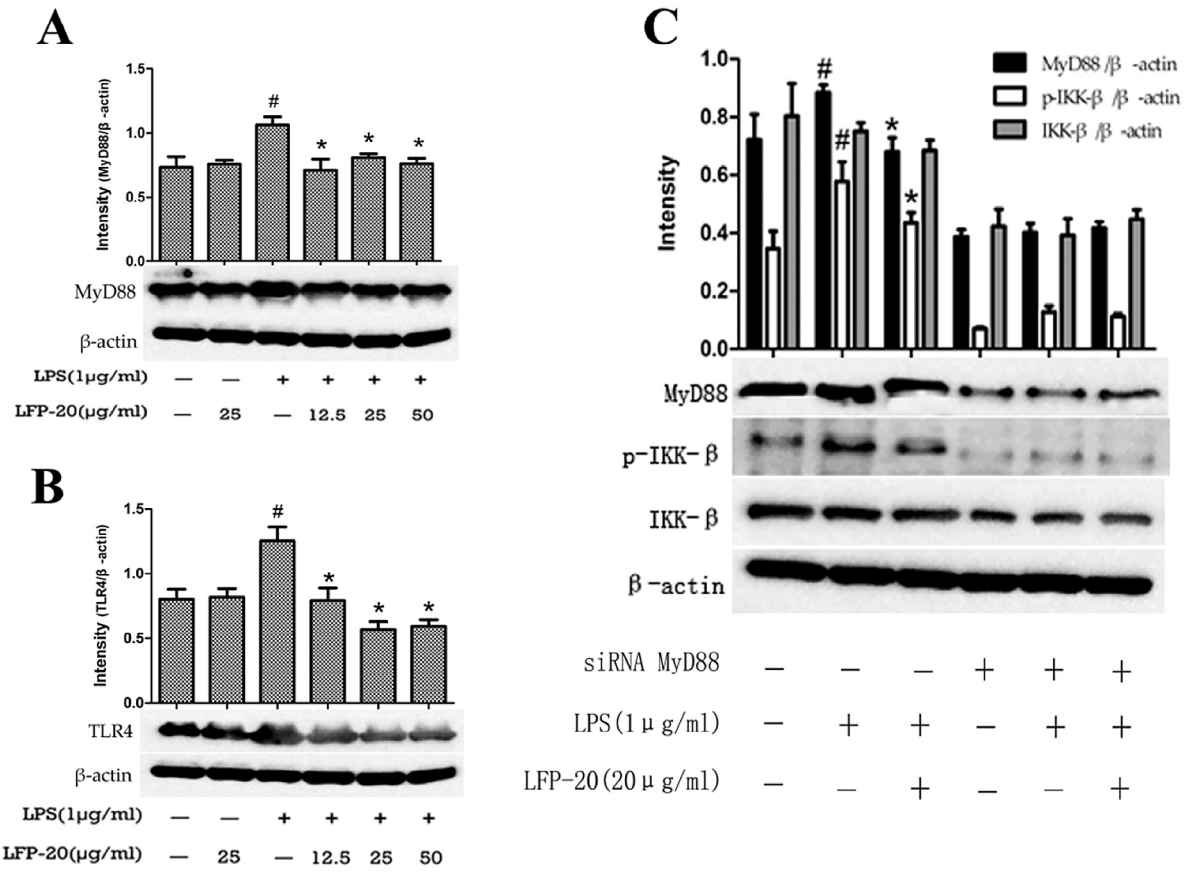

Fig. 5. LFP-20 inhibited LPS-induced IKK-β activation in an MyD88-dependent signaling mechanism. (A) Effect of LFP-20 on LPS-induced activation of MyD88. (B) Effect of LFP-20 on LPS-induced activation of TLR4 expression. The pig alveolar macrophage cell-line 3D4/2 was incubated for 3 h with medium only or 1 μg/mL LPS in the absence or presence of LFP-20 (at concentrations of 12.5, 25, or 50 μg/mL). (C) Effect of LFP-20 on LPS-induced activation of MyD88, IKK-β degradation and IKK-β phosphorylation in MyD88 silenced or non-silenced pig alveolar macrophages. The pig alveolar macrophage cell-line 3D4/2 was transfected with 1 μg/mL siRNA by Lipofectamine-2000, and 6 h after transfection, the cells were treated for 3 h with/without LFP-20 and/or LPS at the indicated concentrations. Protein expression was determined by Western blot assay. β-Actin was used as an internal loading control. Image J software was used to quantify the density of the protein bands. Results are given as mean ± SEM. Differences between groups were determined by one-way ANOVA followed by Duncan's post-hoc analysis (n = 3). $^{\#}p < 0.05$ as compared to the control group, and $^{*}p < 0.05$ as compared to the LPS-treated group.

presence of LFP-20 was decreased as compared with cells treated with LPS alone (Fig. 4B).

3.4. LFP-20 inhibited LPS-induced IKK-β activation in an MyD88-dependent signaling pathway

We further analyzed the importance of the MyD88-dependent pathway in LPS-mediated signaling in pig alveolar macrophages. We found that LPS ttreatment up-regulated MyD88 expression, while incubation with LFP-20 inhibited the LPS-induced increase in MyD88 (Fig. 5A). Furthermore, as shown in Fig. 5C, the level of MyD88, IKK-β and phospho-IKK-β expression in MyD88-silenced macrophages was significantly lower than that found in control cells. However, this outcome differed from that of LPS-induced phosphorylation levels of IKK-β, which was attenuated by LFP-20 in non-silenced macrophages. Under these conditions, we observed that LPS, in the presence of LFP-20 treatment, failed to markedly alter the levels of phospho-IKK-β expression as compared to stimulation with LPS alone in MyD88 silenced macrophages.

In addition, Western blot analysis indicated that LPS enhanced TLR4 expression; however, treatment with LFP-20 inhibited TLR4 expression dose-dependently in pig alveolar macrophages (Fig. 5B).

3.5. The anti-inflammatory effcets of LFP-20 in vivo

Next, we measured whether LFP-20 reduced the accumulation of pro-inflammatory cytokines in mice following exposure to LPS. We injected 10 mg/kg mouse weight LPS into male C57BL/6 mice that were pre-treated with or without LFP-20, and then measured serum TNF-α, IL-6, and IL-1β levels 6 h later. The results showed that the group injected with LFP-20 and LPS had significantly reduced levels of TNF-α, IL-6, and IL-1β as compared with the group treated with LPS alone (Fig. 6). This result demonstrated that LFP-20 inhibited LPS-stimulated cytokine secretion *in vivo*.

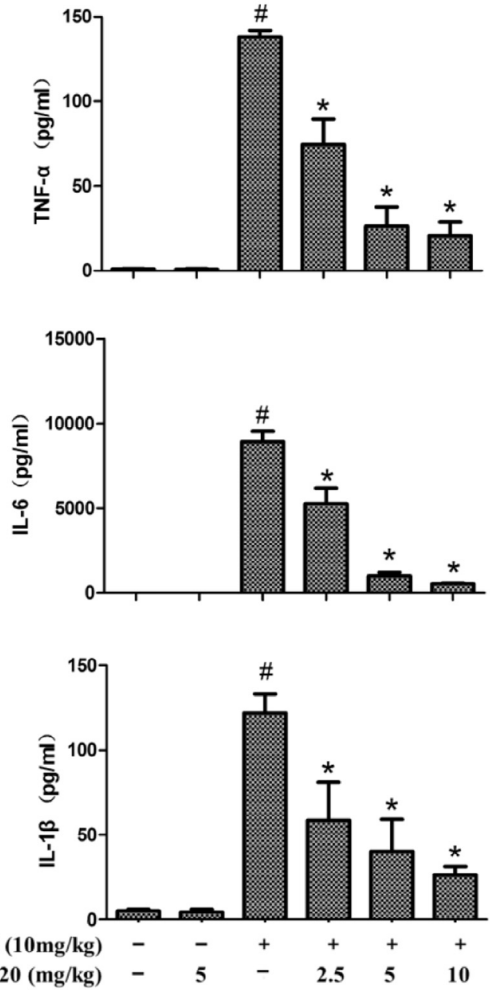

Fig. 6. LFP-20 inhibited TNF-α, IL-6, and IL-1β secretion in LPS-stimulated mice. Different concentrations of LFP-20 were injected i.p. into male C57BL/6 mice once daily for 6 days, whereas the control and LPS-treated groups were i.p. injected with an equal volume of sterile saline. On day 6, mice in the LPS and LFP-20 plus LPS treated groups were i.p. injected with LPS (at a concentration of 10 mg/kg mouse weight) 1 h after LFP-20 or saline treatment. The remaining groups were injected with an equal volume of saline. All mice were sacrificed 6 h after intraperitoneal injection of LPS or saline control. Blood was centrifuged at 3000 rpm for 10 min at room temperature, and serum cytokines were assayed by ELISA. Results are given as mean ± SEM. Differences between groups were determined by one-way ANOVA followed by Duncan's post-hoc analysis (n = 12). $^{\#}p < 0.05$ as compared to the control group, and $^{*}p < 0.05$ as compared to the LPS-treated group.

4. Discussion

In a previous study, the potentially active site of the porcine, bovine, and human lactoferrin peptide was identified through sequence-homologous clustering. Of these peptide sequences, LFP-20 was two amino acids shorter within its cyclic domain than LF that was derived from other species. This form of LF exhibited moderate anti-microbial activity against *Escherichia coli*, *Staphylococcus aureus*, and *Candida albicans* in a mechanism that directly led to cell wall disruption and outer membrane breakdown (Chen et al., 2006). In addition to exerting direct anti-microbial effects, the potential for various lactoferrin peptides as activators of immune-related cellular functions and modulators of the host response to endogenous and exogenous mediators has not been fully investigated. Lactoferrin peptide has both physical and chemical properties that protect against oxidative damage (Ye et al., 2000) and suppress inflammatory cytokine production by interfering with the NF-κB signaling pathway (Inubushi et al., 2012). Kuhara et al. discovered the anti-inflammatory activity of orally administered bovine LF using several mouse models of hepatitis (Kuhara et al., 2014).

The endotoxin-neutralizing activity was a property of cationic peptides (Guo et al., 2005; Rosenfeld et al., 2006). The mechanism may be dependent on the binding between the polycationic peptides and the hydrophobic interaction (Hirsch et al., 2008). Therefore, in some cases, studies attributed the suppressive effects of cationic peptides in the immune response to peptide-LPS binding (Motzkus et al., 2006; Pingel et al., 2008). In our study, the involvement of the anti-inflammtory activities of LFP-20 was independent of LFP-20-LPS binding activity and supported by the results that were obtained following sequential cell treatment with LFP-20 (Fig. 3A, B) and the alternative effects seen with PMB, a cyclic hydrophobic peptide known to bind LPS (Semple et al., 2011) and decreased TNF-α release (Fig. 3D). Overall, these results suggest that in addition to inactivating LPS through the binding activity of the LFP-20-LPS binding activity, LFP-20 also modulated selected cellular pathways and altered LPS-mediated inflammatory responses by its direct effects on macrophages.

In the current study, we found that LFP-20 could effectively reduce the LPS-induced production of TNF-α, IL-6, and IL-1β *in vitro* as well as *in vivo* (Figs. 2 A–F and 6). Various inflammatory diseases involve the over-expression of pro-inflammatory cytokines like TNF-α, IL-6, and IL-1β via NF-κB pathways in macrophages (Moynagh, 2005; Tak and Firestein, 2001). We therefore determined the effects of LFP-20 on NF-κB signaling. The results showed that the expression levels of NF-κB (p65) were effectively suppressed by LFP-20 upon LPS stimulation (Fig. 4A). We also showed that LFP-20 inhibited LPS-induced activation of NF-κB signaling as indicated by reduced phosphorylation of IKK-β (Fig. 4C). These outcomes indicate that

LFP-20 suppressed LPS-induced activation of NF-κB signaling, and did so in a way that likely resulted in reduced production of pro-inflammatory cytokines. In addition, the activation of MAPK pathways regulates gene transcription of inflammatory responses by activating downstream cytosolic proteins and nuclear transcription factors such as NF-κB (Diao et al., 2014). We thus determined the effects of LFP-20 on LPS-stimulated activation of MAPKs, such as p38, and p-c-Jun.

In our study, we found that LFP-20 suppressed LPS-induced activation of p38 and p-c-Jun (Fig. 4B), indicating that the inhibitory effects of LFP-20 on pro-inflammatory cytokine secretion were associated with p38 and c-Jun signaling.

Next, we determined the activation of MyD88, an upstream protein of IKK-β and MAPK, and we found that incubation with LFP-20 inhibited LPS-induced upregulation of MyD88 (Fig. 5A). Interestingly, this differed from the LPS-induced phosphorylation level of IKK-β, which was attenuated by LFP-20 in non-silenced macrophages. Under these conditions, LFP-20 did not significantly inhibit LPS-induced IKK-β phosphorylation in MyD88 siRNA-treated pig alveolar macrophages (Fig. 5C). These data demonstrate that treatment with LFP-20 has the potential to directly influence MyD88 levels by blocking its interactions with other signaling molecules in activated macrophages. The pattern-recognition receptor TLR-4 is activated in various inflammatory diseases; moreover, LPS directly binds with TLR4 (Joh and Kim, 2010). Western blot analysis indicated that treatment with LFP-20 inhibited TLR4 expression that was otherwise enhanced by LPS in a dose-dependent manner in pig alveolar macrophages (Fig. 5B). However, the inhibitory effects of LFP-20 against the binding activity of LPS to TLR4 were not investigated. LFP-20 potentially inhibited the binding of LPS to TLR4 in pig alveolar macrophages. The extracellular LPS-binding activity of cationic peptides of LFP-20 might also contribute to the suppression of TLR4, although it does not play a pivotal role in anti-inflammatory effects.

In conclusion, we demonstrated that LFP-20 attenuated the LPS-induced release of pro-inflammatory factors that were probably associated with MyD88/NF-κB and MyD88/MAPK signaling pathways. This study not only provides increased supporting evidence that LFP-20 exerts anti-inflammatory activity in macrophages, but also provides additional insights into the potential use of LFP-20 as a therapeutic drug for LPS-mediated sepsis.

Acknowledgements

This work was supported by National Natural Science Foundation of China (31172435).

References

Balkwill, F., Mantovani, A., 2001. Inflammation and cancer: back to Virchow? Lancet 357, 539–545.
Bellamy, W., Takase, M., Wakabayashi, H., Kawase, K., Tomita, M., 1992. Antibacterial spectrum of lactoferricin-b, a potent bactericidal peptide derived from the n-terminal region of bovine lactoferrin. J. Appl. Bacteriol. 73, 472–479.
Bellamy, W., Wakabayashi, H., Takase, M., Kawase, K., Shimamura, S., Tomita, M., 1993. Killing of candida-albicans by lactoferricin-b, a potent antimicrobial peptide derived from the n-terminal region of bovine lactoferrin. Med. Microbiol. Immunol. (Berl) 182, 97–105.
Chen, B.C., Lin, W.W., 2001. PKC- and ERK-dependent activation of I kappa B kinase by lipopolysaccharide in macrophages: enhancement by P2Y receptor-mediated CaMK activation. Br. J. Pharmacol. 134, 1055–1065.
Chen, H.L., Yen, C.C., Lu, C.Y., Yu, C.H., Chen, C.M., 2006. Synthetic porcine lactoferricin with a 20-residue peptide exhibits antimicrobial activity against Escherichia coli, Staphylococcus aureus, and Candida albicans. J. Agric. Food Chem. 54, 3277–3282.
Diao, Y., Xin, Y., Zhou, Y., Li, N., Pan, X., Qi, S., et al., 2014. Extracellular polysaccharide from Bacillus sp strain LBP32 prevents LPS-induced inflammation in RAW 264.7 macrophages by inhibiting NF-kappa B and MAPKs activation and ROS production. Int. Immunopharmacol. 18, 12–19.
Du, X., Poltorak, A., Silva, M., Beutler, B., 1999. Tlr4, transducing subunit of the sole mammalian LPS receptor, is the limiting factor in macrophage endotoxin signaling. Blood 94, 584A.
Guo, Y.B., Zheng, J., Zhou, G., Lv, G.F., Wang, L.X., Wei, G., et al., 2005. A synthesized cationic tetradecapeptide from hornet venom kills bacteria and neutralizes lipopolysaccharide in vivo and in vitro. Biochem. Pharmacol. 70, 209–219.
Han, F.F., Gao, Y.H., Luan, C., Xie, Y.G., Liu, Y.F., Wang, Y.Z., 2013. Comparing bacterial membrane interactions and antimicrobial activity of porcine lactoferricin-derived peptides. J. Dairy Sci. 96, 3471–3487.
Hirsch, T., Metzig, M., Niederbichler, A., Steinau, H.-U., Eriksson, E., Steinstraesser, L., 2008. Role of host defense peptides of the innate immune response in sepsis. Shock 30, 117–126.
Hoebe, K., Du, X., Georgel, P., Janssen, E., Tabeta, K., Kim, S.O., et al., 2003. Identification of Lps2 as a key transducer of MyD88-independent TIR signalling. Nature 424, 743–748.
Inubushi, T., Kawazoe, A., Miyauchi, M., Kudo, Y., Ao, M., Ishikado, A., et al., 2012. Molecular mechanisms of the inhibitory effects of bovine lactoferrin on lipopolysaccharide-mediated osteoclastogenesis. J. Biol. Chem. 287, 23527–23536.
Joh, E.-H., Kim, D.-H., 2010. A sensitive liquid chromatography-electrospray tandem mass spectrometric method for lancemaside A and its metabolites in plasma and a pharmacokinetic study in mice. J. Chromatogr. B. Analyt. Technol. Biomed. Life Sci. 878, 1875–1880.
Kawai, T., Adachi, O., Ogawa, T., Takeda, K., Akira, S., 1999. Unresponsiveness of MyD88-deficient mice to endotoxin. Immunity 11, 115–122.
Korhonen, R., Lahti, A., Kankaanranta, H., Moilanen, E., 2005. Nitric oxide production and signaling in inflammation. Curr. Drug Targets Inflamm. Allergy 4, 471–479.
Kuhara, T., Tanaka, A., Yamauchi, K., Iwatsuki, K., 2014. Bovine lactoferrin ingestion protects against inflammation via IL-11 induction in the small intestine of mice with hepatitis. Br. J. Nutr. 111, 1801–1810.
Kyriakis, J.M., Avruch, J., 2001. Mammalian mitogen-activated protein kinase signal transduction pathways activated by stress and inflammation. Physiol. Rev. 81, 807–869.
Lee, W., Yoo, H., Kim, J.A., Lee, S., Jee, J.-G., Lee, M.Y., et al., 2013. Barrier protective effects of piperlonguminine in LPS-induced inflammation in vitro and in vivo. Food Chem. Toxicol. 58, 149–157.
Libby, P., 2006. Inflammation and cardiovascular disease mechanisms. Am. J. Clin. Nutr. 83, 456S–460S.
Livak, K.J., Schmittgen, T.D., 2001. Analysis of relative gene expression data using real-time quantitative PCR and the 2(T)(–Delta Delta C) method. Methods 25, 402–408.
Medzhitov, R., 2001. Toll-like receptors and innate immunity. Nat. Rev. Immunol. 1, 135–145.
Motzkus, D., Schulz-Maronde, S., Heitland, A., Schulz, A., Forssmann, W.-G., Juebner, M., et al., 2006. The novel beta-defensin DEFB123 prevents lipopolysaccharide-mediated effects in vitro and in vivo. FASEB J. 20, 1701.
Moue, M., Tohno, M., Shimazu, T., Kido, T., Aso, H., Saito, T., et al., 2008. Toll-like receptor 4 and cytokine expression involved in functional immune response in an originally established porcine intestinal epitheliocyte cell line. Biochim. Biophys. Acta 1780, 134–144.
Moynagh, P.N., 2005. The NF-kappaB pathway. J. Cell Sci. 118, 4589–4592.
O'Keefe, J.H., Gheewala, N.M., O'Keefe, J.O., 2008. Dietary strategies for improving post-prandial glucose, lipids, inflammation, and cardiovascular health. J. Am. Coll. Cardiol. 51, 249–255.
Pingel, L.C., Kohlgraf, K.G., Hansen, C.J., Eastman, C.G., Dietrich, D.E., Burnell, K.K., et al., 2008. Human beta-defensin 3 binds to hemagglutinin B (rHagB), a non-fimbrial adhesin from Porphyromonas gingivalis, and attenuates a pro-inflammatory cytokine response. Immunol. Cell Biol. 86, 643–649.
Rosenfeld, Y., Papo, N., Shai, Y., 2006. Endotoxin (lipopolysaccharide) neutralization by innate immunity host-defense peptides – Peptide properties and plausible modes of action. J. Biol. Chem. 281, 1636–1643.
Scherle, P.A., Jones, E.A., Favata, M.F., Daulerio, A.J., Covington, M.B., Nurnberg, S.A., et al., 1998. Inhibition of MAP kinase kinase prevents cytokine and prostaglandin E-2 production in lipopolysaccharide-stimulated monocytes. J. Immunol. 161, 5681–5686.
Semple, F., MacPherson, H., Webb, S., Cox, S.L., Mallin, L.J., Tyrrell, C., et al., 2011. Human beta-defensin 3 affects the activity of pro-inflammatory pathways associated with MyD88 and TRIF. Eur. J. Immunol. 41, 3291–3300.
Tak, P.P., Firestein, G.S., 2001. NF-kappa B: a key role in inflammatory diseases. J. Clin. Invest. 107, 7–11.
Tomita, M., Bellamy, W., Takase, M., Yamauchi, K., Wakabayashi, H., Kawase, K., 1991. Potent antibacterial peptides generated by pepsin digestion of bovine lactoferrin. J. Dairy Sci. 74, 4137–4142.
Wang, C., Deng, L., Hong, M., Akkaraju, G.R., Inoue, J., Chen, Z.J.J., 2001. TAK1 is a ubiquitin-dependent kinase of MKK and IKK. Nature 412, 346–351.
Weingartl, H.M., Sabara, M., Pasick, J., van Moorlehem, E., Babiuk, L., 2002. Continuous porcine cell lines developed from alveolar macrophages: partial characterization and virus susceptibility. J. Virol. Methods 104, 203–216.
Yamamoto, M., Sato, S., Hemmi, H., Hoshino, K., Kaisho, T., Sanjo, H., et al., 2003. Role of adaptor TRIF in the MyD88-independent toll-like receptor signaling pathway. Science 301, 640–643.
Ye, X.Y., Wang, H.X., Liu, F., Ng, T.B., 2000. Ribonuclease, cell-free translation-inhibitory and superoxide radical scavenging activities of the iron-binding protein lactoferrin from bovine milk. Int. J. Biochem. Cell Biol. 32, 235–241.